Oxygen and Iron Production By Electrolytic Smelting of Lunar Soil

R.O. Colson and L.A. Haskin
Dept. of Earth and Planetary Science
Washington University

INTRODUCTION:

Oxygen, present in abundance in nearly all lunar materials, theoretically can be extracted by molten silicate electrolysis from any known lunar rock. Derivation of oxygen by this method has been amply demonstrated experimentally in silicate melts of a variety of compositions (e.g. Bockris et al., 1952a,b, Simnad et al., 1954, Oppenheim 1968, 1970, Kesterke, 1971, and Lindstrom and Haskin, 1979). In our previous work, we have defined further the conditions necessary to optimize oxygen production by silicate melt electrolysis. We have demonstrated that the conductivity of silicate melts and efficiencies of O_2 production are sufficiently high to permit practical electrolysis of lunar materials (Haskin et al., 1991, Colson and Haskin, 1990). We have measured the dependence of conductivity on melt composition and the dependence of efficiency (fraction of current that produces oxygen) on FeO concentration in the melt. We have studied the kinetics of cathodic and anodic reactions and found them suitable for electrolysis (Haskin and Semkow, 1985).

Our work of the past year, supplementing these previous results, can be divided into three categories. These categories are the following: 1) measurement of solubilities of metals (atomic) in silicate melts; 2) electrolysis experiments under various conditions of temperature, container material, electrode configuration, current density, melt composition, and sample mass (100 to 2000 mg) measuring energy required and character of resulting products; 3) and theoretical assessment of compositional requirements for steady state operations of an electrolysis cell.

METAL SOLUBILITIES:

Solubility of species in the atomic state in silicate melts can potentially decrease the O_2 production efficiency because Fe° and Si° produced at the cathode will dissolve in the melt and be reoxidized at the cathode, producing Fe^{2+} and Si(IV) rather than oxygen. We have measured the solubilities of Ni°, Co° and Ir° in silicate melts and determined an upper limit for Fe° solubility. Results suggest that solubility of each of these species is <0.2 wt%. By analogy with the concentrations of Fe^{2+} required to reduce O_2 efficiency significantly (about 2-5 wt%), we conclude that metals dissolved in the silicate melt will not greatly affect production efficiency.

We measured the solubility of Ir to be approximately 200 ppm. A less rigorous measurement for Pt indicated its solubility might also be as high as 100's of ppm. This value is substantially higher than that we reported last year and, depending on how quickly the Pt equilibrates with the melt, suggests that Pt might be too soluble to be considered as an inert electrode material in electrolysis as we have suggested previously. If the silicate melt equilibrates rapidly with the Pt and is actually that high, 20% of the anode would be gone after a feedstock flowthrough of only ~1000 times its mass. Also, other observations suggest that the Pt anodes are maintained in a state of dynamic equilibrium in which the Pt is oxidized at the electrode but quickly reduced by the silicate melt as the oxidized Pt migrates away from the electrode. This results in a substantially roughened anode surface (Fig. 1). Over an extended period of time this process might destroy the Pt anode. At potentials substantially higher than the 0 to 10 volt range we are working in, the Pt anode is completely oxidized and melts. Our previous experience has indicated no tendency for Pt anodes to erode or fail, but anode stability is so important that we must learn whether there are conditions that lead to anode failure.

A12- 1Ch - near anode

Fig. 1 Platinum globs in melt near the Pt anode after electrolysis, suggesting that the Pt anode is not inert during electrolysis. Backscattered Electron Image (BEI).

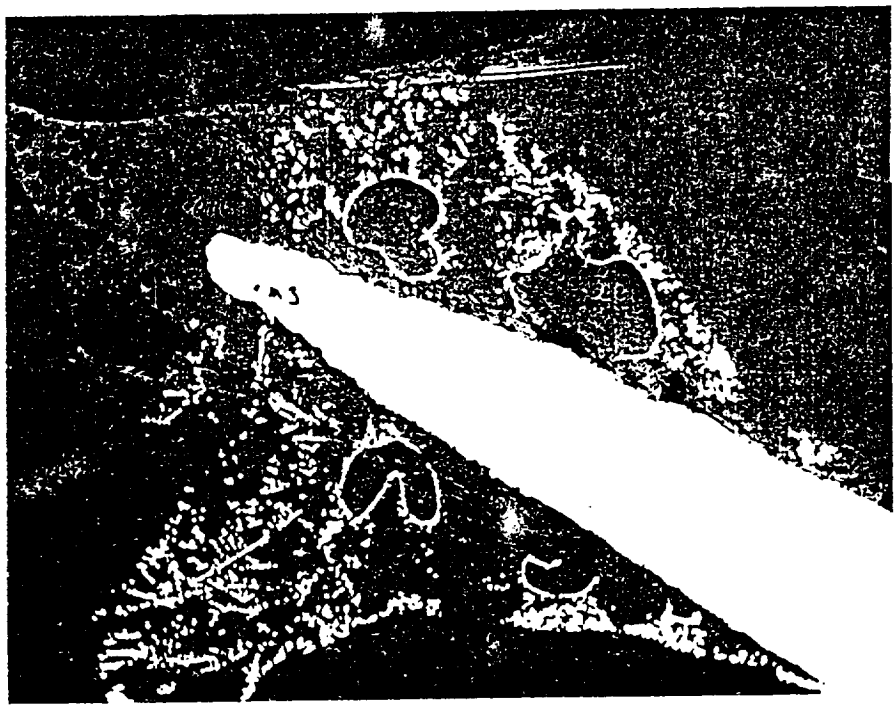

A12 - 1Cg

Fig. 2 Iron dendrites that form near the cathode tend to short the cell at temperatures below the melting point of the metal. Note "bubbles" of iron. (BEI)

ELECTROLYSIS EXPERIMENTS:

In an effort to measure energies required for electrolysis, characterize product form and composition, and identify potential problems with the electrolysis process, we have done a series of electrolysis experiments. These are of two types. The first uses 50-100mg of silicate material held by surface tension onto Pt loops about 5mm in diameter. These loops act as anodes. A second Pt electrode passes through the melt inside the Pt loop of each experiment. The composition of silicate melt used in these experiments ranged from FeO-poor (no FeO) to FeO-rich (18% FeO). Some compositions were similar to lunar soils. The second type uses 1 to 2 g of silicate material in spinel ($MgAl_2O_4$) crucibles. These crucibles were 8mm inside diameter by 14mm inside length. The cathode was a Pt coil that entered the crucible through a small hole drilled in the bottom. The Pt anode entered the crucible from the top. The cathode and anode were placed about 0.5cm apart. The composition used in the experiments were chosen to represent possible steady state compositions plus a few percent lunar soil.

Product character

We have identified the solid products of the electrolysis. They are metal (produced at the cathode) and spinel (which exsolves from the melt as SiO_2 and FeO are removed from it). At potentials less than about one volt, only Fe metal is produced at the cathode. At temperatures less than the Fe melting temperature, the Fe forms dendrites that tend to short the electrolytic cell (Fig. 2). The dendrites expand into the melt as a "bubble" of metal, with melt in the interior of the bubble depleted in Fe and the exterior rich in Fe.

At higher potentials (greater than 1 volt), both Si and Fe are produced at the cathode (with minor Ti, Cr, Mn, and other trace constituents). We have observed the coexistence of as many as three metal phases (Colson, 1990). We associate these metal phases with the c, a, and melt phases in the Fe-Si system (Lyman, 1973). The highest concentration of Si in metal that we have observed is about 10wt%. In most cases, this is less than the amount of Si expected based on thermodynamic calculations. Metal more distant from the cathode has substantially less Si than metal near the cathode, suggesting that the Si in the Si-Fe alloy is reacting with the melt to form Fe in the metal and Si(IV) dissolved in the melt.

In the 50 to 100mg experiments, the metal product is often broken into small particles and mixed throughout the sample by stirring caused by the bubbles that form and escape at the anode. Substantial dissemination of metal in melt is seen in Fig. 3. This mixing probably enhances the reaction of Si with the melt. Mixing of metal back into the melt was not observed in the larger scale experiments done in spinel crucibles.

Spinel ($MgAl_2O_4$) is observed to precipitate near the cathode in experiments with low FeO concentrations (<5%) run in spinel crucibles (in which the melt is saturated with spinel). This spinel sometimes forms a sheath around the cathode, increasing the cell resistance (Fig 4). In experiments containing Fe and Cr, an Fe-Cr rich spinel is observed to form near the cathode. Based on thermodynamic calculations, spinel is expected to precipitate as SiO_2 is removed from the melt by electrolysis.

Spinel crucibles appear to be stable, as expected, in a spinel-saturated silicate melt. After several hours of contact with the melt, the spinel does not deteriorate (Fig. 4). The stringers of melt invading the spinel in Fig. 4 probably have followed fractures induced by the thermal shock caused by repeatedly putting the sample in the furnace and taking it out.

One spinel crucible nearly failed during actual electrolysis. Figure 5 shows the spinel crucible wall after only forty minutes of electrolysis. The spinel is substantially corroded and invaded by the melt. This destruction of the spinel occurred in the immediate vicinity of the cathode suggesting a reaction with a cathodic product. The vesicles in the vicinity of the cathode, also seen in Fig. 5, suggest the formation of a gas phase at the cathode. This gas appears to be a cathodic product, and may actually have attacked the spinel wall. The presence of vapor-deposited Pt in the vesicles seen in the figure suggests that this gas mobilized Pt. We have

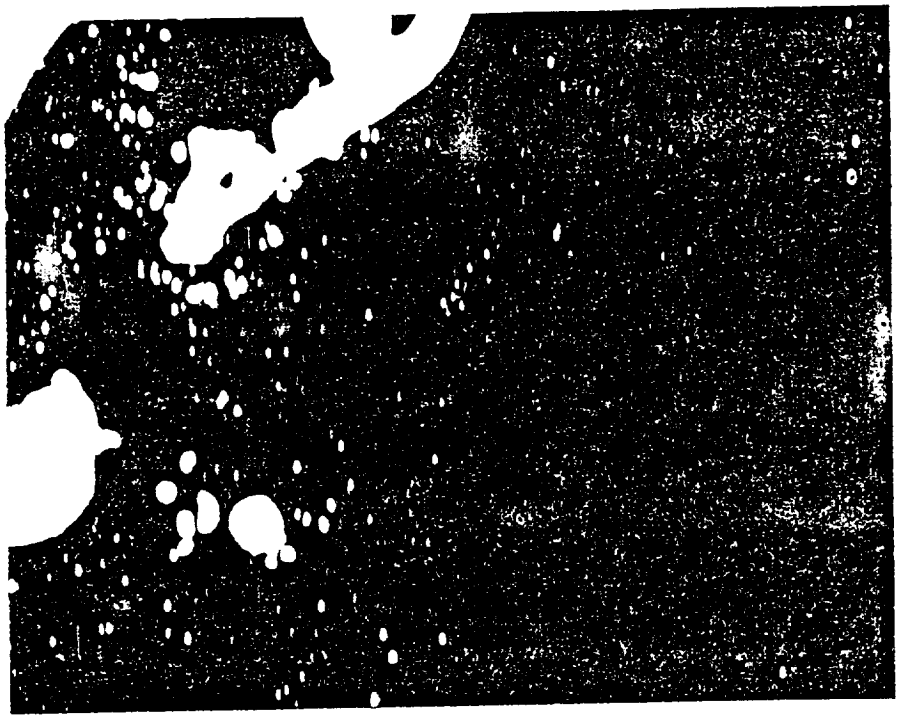

A12 - 1ci

Fig. 3 Metal disseminated in glass as small metal beads. This is probably caused by violent mixing of the small sample by oxygen bubbles formed at the anode. (BEI)

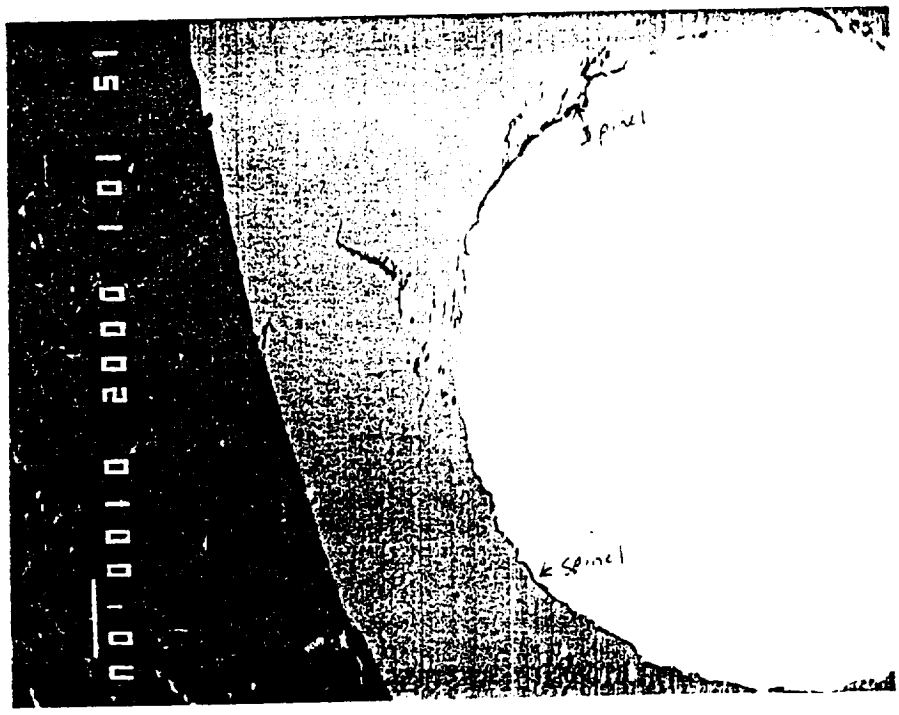

Elec55 6

Fig. 4 Spinel is the darker phase forming a narrow sheath around the bright Ir cathode. Spinel also forms the crucible wall seen on the left. The spinel crucible does not appear to be corroded by the melt. (BEI)

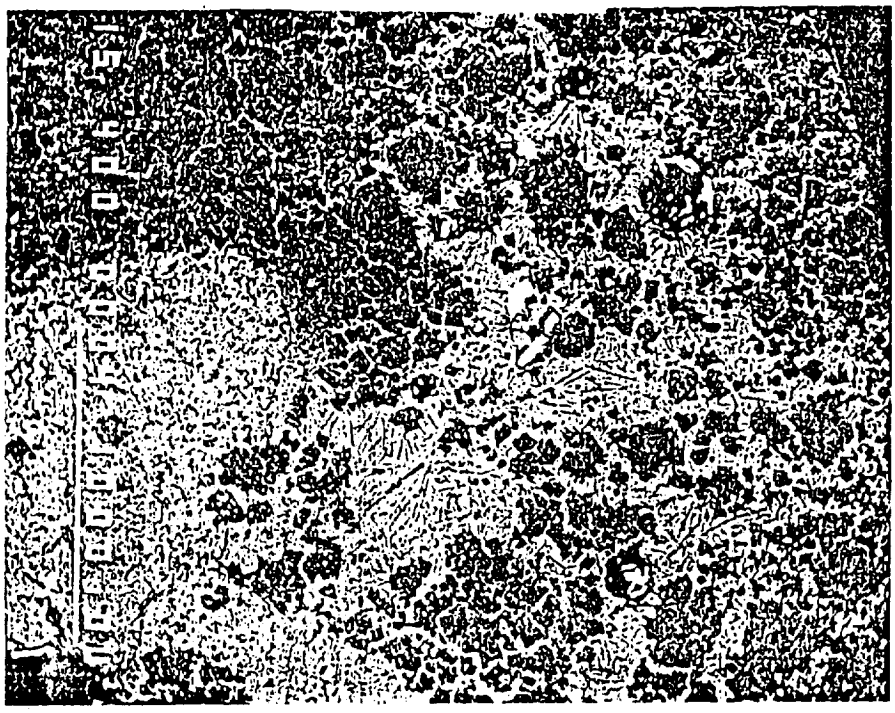

Elec5520

Fig. 5 Darker areas are pieces of the spinel crucible corroded and invaded by the lighter colored melt. Black circles are vesicles partially filled with bright Pt crystals. This picture is taken near the base of the crucible and near the cathode. This picture is evidence that the spinel crucible is corroded by a gaseous product of electrolysis. (BEI)

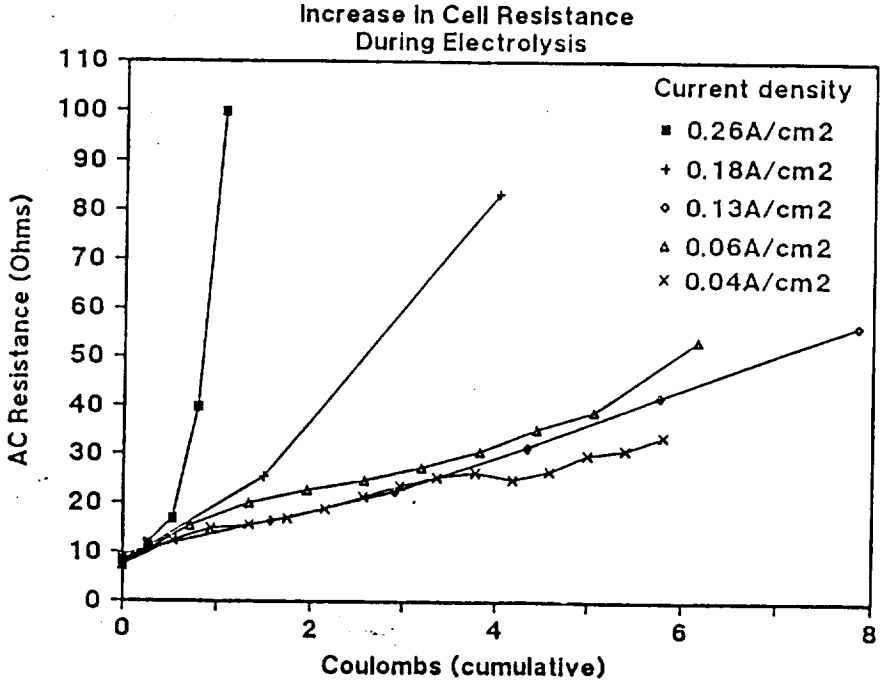

Fig. 6 Dependence of AC resistance on total current for experiments in composition SS1. We believe that the sharp increase in resistance during electrolysis is due to frothing of the melt, resulting from failure of the oxygen generate at the anode to escape sufficiently quickly from the melt.

determined that the gas forms at the cathode in air, CO_2, and argon atmospheres when the only constituents of the melt are SiO_2, CaO, MgO, and Al_2O_3, or when FeO is present as well. We have found the gas to form at the cathode using either a Pt or Ni cathode. We speculate that the gas may contain a silicon monoxide species analogous to carbonyls. However, this problem requires further study to determine what the gas is and what effect, if any, it has on the spinel container and how any effect can be minimized.

Energy measurements

In the 1 to 2 g experiments, cell resistance during electrolysis (from which energy use can be calculated by energy = I^2Rtime+theoretical energy to reduce melt) was measured as a function of current density, depth of anode in the melt, and melt composition. Results are shown in Figs. 6-8.

The sharp and progressive increase in resistance during electrolysis is due primarily to frothing of the melt caused when bubbles generated cannot escape sufficiently quickly. Using lower current densities or placing the anode at different depths in the melt yields little improvement (Figs. 6 and 7). We also tried different types of anodes (i.e. straight wire rather than a coil, Pt screen, and more or less tightly coiled Pt anodes) without much improvement. We tried "stirring" the melt by moving the anode up and down about 1-2mm at about one cycle every 2 seconds but this caused the frothing melt to be quickly lost out the top of the crucible.

Lower concentrations of SiO_2 and Al_2O_3 result in lower viscosities (Bottinga and Weill, 1972) and surface tension (Walker and Mullins, 1981). At lower concentrations of these species, the frothing does not occur (Fig. 8). Frothing will probably constrain us to use lower SiO_2, Al_2O_3 melts (<about 55% $SiO_2+Al_2O_3$) as the steady state composition of the cell. However, it is possible that in larger pots, in which the surface energy between the crucible and the melt is not as important, the frothing problem may not be significant.

The use of the lower $SiO_2+Al_2O_3$ melt as the steady state "flux" in the 1 to 2 g experiments results in an energy requirement for the electrolysis less than 30% greater than the theoretical minimum (presuming that 85% or more of the current goes to producing oxygen, after Haskin et al., 1991). This very low energy requirement is substantially less than has been suggested for most other processes, which require 2 to 4 times the theoretical energy (Colson and Haskin, 1990) and is less than the energy requirement we calculated on theoretical grounds for batch electrolysis (Haskin et al., 1991).

However, Haskin et al. (1991) presumed a current density of about 1 A/cm^2 whereas the experiments in composition SS2 (the lower $SiO_2+Al_2O_3$ experiments) in which no frothing occurred had a current density of about 0.1 A/cm^2. At higher current densities in the vicinity of 0.8 to 1 A/cm^2, resistance varied erratically, as though frothing periodically increased and dissipated, and energy requirements were correspondingly higher.

COMPOSITIONAL REQUIREMENTS OF STEADY STATE:

Several considerations must be made in assessing the ideal composition of the steady state melt maintained as a "flux" in the electrolysis cell. These include the need to minimize the energy requirements of electrolysis (generally, decreasing SiO_2, Al_2O_3, and FeO improves efficiency of the process; Haskin et al., 1991, and Taylor et al., 1991), the need to provide a composition in which the chosen container and electrode materials are not consumed (for example, spinel as a container or electrode requires a melt in equilibrium with it; Colson and Haskin, 1990, and McCullough and Mariz, 1990), and the composition of the feedstock. The variables we can use to control the steady state composition include the feedstock composition (which can presumably be varied within certain limits), the composition of the metal product (which can be varied by adjusting cell potential and feedstock flow-through rate), and the temperature (which places constraints on the composition of a melt in equilibrium with a container or electrode material).

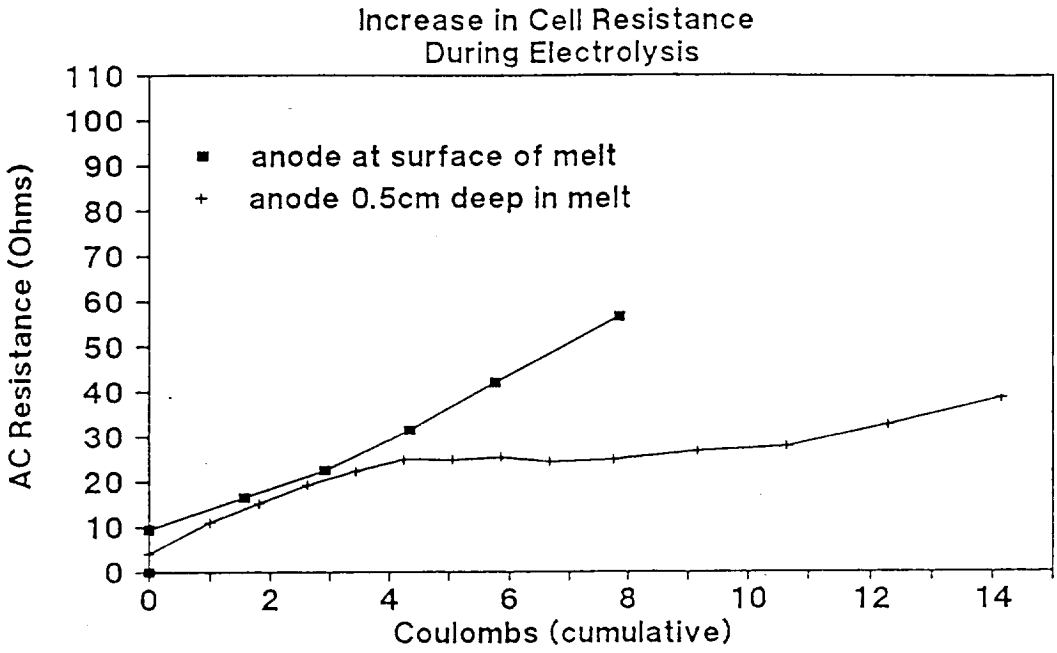

Fig. 7 Dependence of frothing (indicated by increase in resistance with current) on the depth of the anode in the melt for composition SS1.

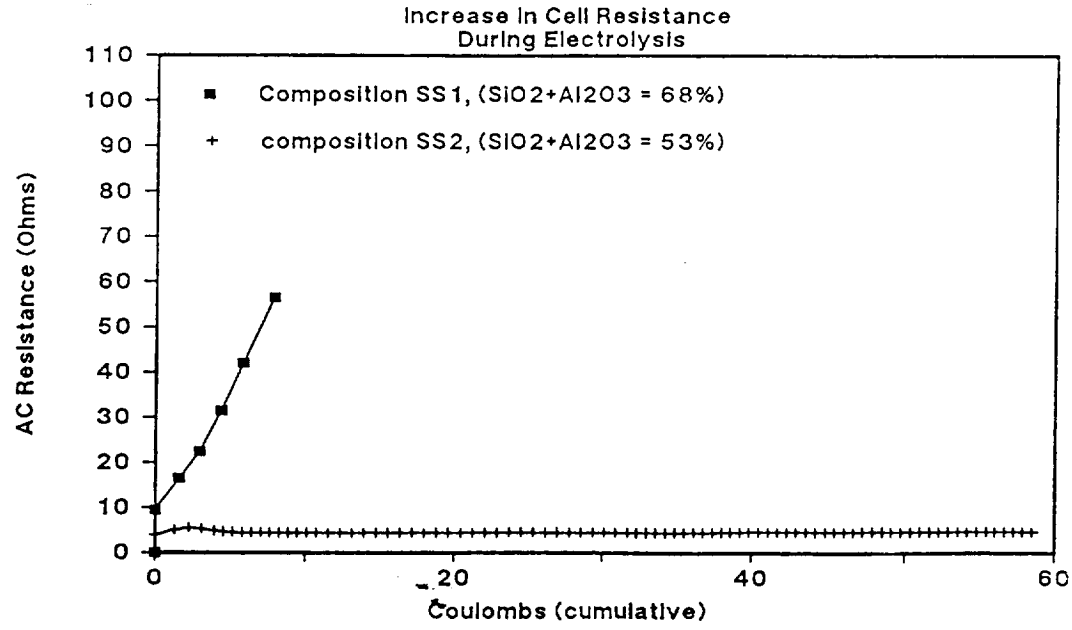

Fig. 8 Dependence of frothing (indicated by increase in resistance with current) on melt composition.

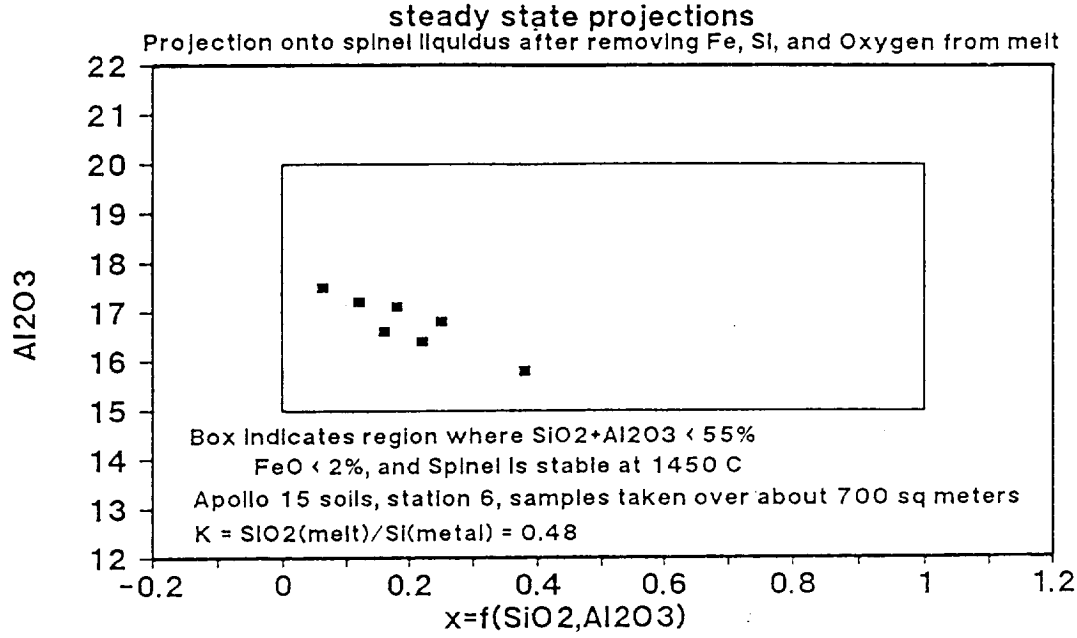

Fig. 9 Theoretical calculation of the steady state melt composition for several Apollo 15, station 6 soil compositions projected onto the spinel liquidus surface, illustrating that for given values of temperature and cell potential, all station 6, Apollo 15 soils in this data set meet the criteria defined in the text for efficient electrolysis and spinel stability. These projections are made by first removing FeO, TiO_2, and SiO_2 from the melt according to the selected value for K, then projecting from spinel onto the surface defined by the spinel liquidus at 1450°C. Data are from Korotev (1987) and Morris et al (1983).

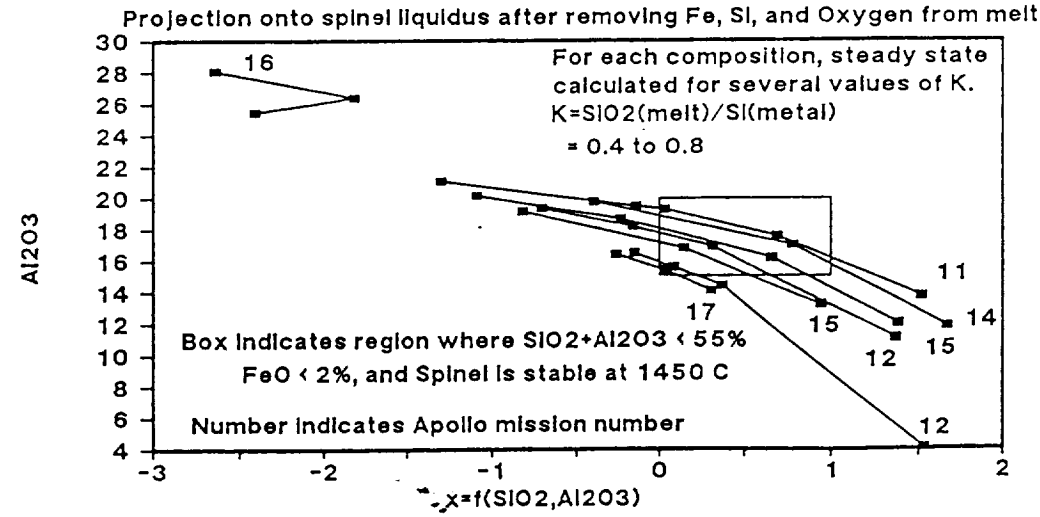

Fig. 10 Illustration that steady state for soils from most Apollo missions can be maintained on the spinel liquidus, and at compositions compatible with efficient electrolysis by adjusting cell potential. Points on the curves represent steady state calculations done for different cell potentials (different values for K). Data are from Taylor (1982).

In the following example, we constrain the steady state concentration of FeO to be less than 2% (to maximize oxygen production/current, Haskin et al, 1991), $SiO_2+Al_2O_3$ to be less than 55% (to minimize frothing and maximize melt conductivity, Haskin et al, 1991, and this report), and the steady state melt to be in equilibrium with spinel ($MgAl_2O_4$). Depending on the potential imposed between the electrodes, and on the residence time of the melt, Si/Fe in the metal product can vary between 0 and Si(melt)/Fe(melt). In this exercise we assume the feedstock achieves equilibrium at the imposed potential. Therefore, the amounts of Fe, Ti, and Si metal produced are defined by K_{Fe} = f(E) = FeO(melt)/Fe(metal), K_{Si} = f(E) = SiO_2(melt)/Si(metal), and K_{Ti} ~ K_{Si}. Here, E is cell potential, and, for this exercise, the activities are approximated by wt% SiO_2 in melt and mole fraction Si or Fe in metal. (This does not constrain the produced molten alloy to be in equilibrium with any solid Fe-Si alloy, as might be desired if a solid Fe-Si metal is used as a cathode.) The amount of spinel removed from the melt is determined from phase equilibria (e.g. pg. 185 in Levin et al, 1969). After a sufficient length of time, the steady state composition is defined by the relationship:

Wt fraction A in Cell = (a-bc)/(1-c)

where a = weight fraction of A in feedstock, b = weight fraction of A in product, and c = weight fraction of feed that yields product.

Two questions are of interest. How much variation can there be in feedstock composition for a given set of electrolysis conditions (temperature, cell potential) without causing the steady state compositions to deviate from the ranges defined above (that is, how sensitive is the process to feedstock variations)? Secondly: How wide a variation in feedstock composition can be accommodated by adjusting temperature and cell potential to maintain the steady state composition within the compositional range defined above (that is, how robust is the process with respect to feedstock composition)?

Figure 9 illustrates that the process is not sensitive to anticipated local variations in feedstock composition. Over a region of about 700 square meters at station 6, Apollo 15, variations in the soil composition are small enough such that the steady states for all compositions are within the range defined above. The axes of Fig. 10 are chosen such that the stability field of spinel at 1450°C can be approximately plotted on the figure. That region of the spinel stability field which also meets the other criteria outlined above is shown by a box on the figure.

When data for more soils from Apollo 15 sampled over several square kilometers are included, they do not all fall within the box. However, by adjusting the value of K (which is a function of cell potential and therefore can be controlled), the steady state arising from these other soil compositions could be brought into the box on the figure. In fact, steady states deriving from many of the soils sampled by the Apollo missions can meet the criteria defined above (Fig. 10), demonstrating the versatility of the electrolysis process with respect to feedstock composition. By adjusting the cell potential, the steady state composition for all the example soils except that from Apollo 16 can meet the combined criteria for high conductivity, low viscosity, high production efficiency, and spinel on the liquidus. We point out that whether or not spinel is ultimately chosen as a container material determines whether the rather stringent criteria of maintaining the steady state composition in equilibrium with spinel is actually required. If some other container is ultimately chosen, some of the above criteria may be relaxed, or may be replaced by others, e.g., if it is desirable to keep some other liquidus phase present. This discussion is given as an example illustrating that the process is versatile with respect to feedstock composition but is not particularly sensitive to variations in feedstock composition over a small region.

Bockris, J. O'M., Kitchener, J. A. and Davies, A. E. (1952a) Electric transport in liquid silicates, Trans. Faraday Soc., 48, pp. 536-548.

Bockris, J. O'M., Kitchener, J. A. Ignatowicz, W. and Tomlinson, J. W. (1952b) Electric conductance in liquid silicates, Trans. Faraday Soc., 48, pp. 75-91.

Bottinga Y. and Weill D. F. (1972) The viscosity of magmatic silicate liquids: a model for calculation, Am. J. Sci., 272, pp. 438-375.

Colson, R. O. (1990) Characterization of metal products of silicate melt electrolysis, Lunar Planet. Sci. XXI, pp. 214-215. The Lunar and Planetary Inst., Houston.

Colson R. O. and Haskin L. A. (1990) Lunar oxygen and metal for use in near-earth space: Magma electrolysis, in Engineering, Construction, and Operations in Space: Vol 1 (ed Johnson, S. W. and Wetzel, J. P.), ASCE New York.

Haskin, L. A., Colson R. O., Lindstrom, D. J., Lewis, R. H. and Semkow, K. W. (1991) Electrolytic smelting of lunar rock for oxygen, iron and silicon, in Lunar Bases and space Activities of the 21st Century (II), Mendell, W. W. (ed.), LPI, in press.

Kesterke D. G. (1971) Electrowinning of oxygen from silicate rocks. U. S. Bureau of Mines Report of Investigations 7587. 10pp.

Korotev R. L., (1987) Mixing levels, the Apennine front soil component, and compositional trends in the Apollo 15 soils, Proc. 17th Lunar Sci. Conf., J. Geophys. Res. 92, E411-E431.

Levin E. M., Robbins C. R., and McMurdie H. F. (eds) (1969) Phase Diagrams for Ceramists, Vol 2, The American Ceramic Society.

Lindstrom D. J. and Haskin L. A. (1979) Electrochemical preparation of useful material from ordinary silicate rocks. in Space Manufacturing Facilities, Gray, J. and Krop C. (eds.) AIAA, pp. 129-134.

Lyman T. (Ed.) (1973) Metals Handbook, Vol. 8, 8th Ed. Metallography, structures and phase diagrams, Am. Soc. for Metals, Metals Park, OH.

McCullough, E. and Mariz, C. (1990) Lunar oxygen production via magma electrolysis, in Engineering, Construction and Operations in Space, Johnson, S. W. and Wetzel, J. P. (eds.) New York: American Soc. Civil Eng. pp. 347-356.

Morris R. V., Score, R., Dardano C., and Heiken G. (1983) Handbook of lunar soils, NASA/JSC publication 67, Houston.

Oppenheim, M. J. (1968) On the electrolysis of molten basalt, Mineral. Mag., 36, pp. 1104-22.

Oppenheim, M. J. (1970) On the electrolysis of basalt, II: experiments in an inert atmosphere, Mineral. Mag., 37, pp. 568-577.

Semkow,K. W. and Haskin L. A. (1985) Concentrations and behavior of oxygen and oxide ion in melts of composition CaO MgO xSiO_2, Geochim. Cosmochim. Acta 49, pp. 1897-1907.

Simnad, M. T., Derge, G. and George, I. (1954) Ionic nature of liquid iron-silicate slags, J. Metals, 6, pp. 1386-1390.

Taylor S. R. (1982) Planetary Science: A lunar perspective, Lunar and Planetary Inst., Houston.

Taylor L. A., Cooper B, McKay D. S., and Colson R. O. (1991) Oxygen production on the moon: Processes for different feedstocks, Metallurgy processing fundamentals: Lunar mining and Processing, Soc. of Mining, Metallurgy, and Exploration (SME) (in press).

Walker, D. and Mullins, Jr., O. (1981) Surface Tension of natural silicate melts from 1,200 -1500 C and implications for melt structure, Contrib. Mineral. Petrol., 76, pp. 455-462.